Supporting Information

Synthesis, crystal structure, DFT/TDDFT calculation, photophysical properties and DNA binding studies of morpholino moiety ligand based two Cu(II) complexes in combination with carboxylates

Aparup Paul,[a] Soumen Mistri,[a] Apurba Bhunia, [a] Soumen Manna,[a] Horst Puschmann,[b] Subal Chandra Manna[*,a]

[a]*Department of Chemistry and Chemical Technology, Vidyasagar University, Midnapore 721102, West Bengal, India, E-mail: scmanna@mail.vidyasagar.ac.in, Fax: (91) (03222) 275329.*

[b]*Department of Chemistry, University of Durham, South Road, Durham DH1 3LE, U.K.*

Table 1S C-H…π interactions in complexes **1** and **2**.

C--H	Cg(J)	H…Cg (Å)	X-H…Cg (º)	X…Cg (Å)
*Complex **1***				
C(10)-H(10A)	Cg(8)→ C(23) - C(24)- C(25) - C(26) -C(27) - C(28)	2.762	161	3.6364(19)
C(12)-H(12A)	Cg(8)→ C(23) - C(24)- C(25) - C(26) -C(27) - C(28)	3.670	122.85	4.28
*Complex **2***				
C(12)-H(12A)	Cg(7) → C(1) - C(2)- C(3)-C(4) - C(5)- C(6)	3.200	133.85	3.95
C(27)-H(27B)	Cg(8) →C(21) -C(22)- C(23)- C(24)-C(25)-C(26)	3.498	108.06	3.91

Table 2S List of selected excitation bands of HL calculated using different functionals (B3LYP, B3PW91, MPW1PW91) [CPCM model in methanolic, basis set, 6-31G (d-p)].

Functional	Wavelength λ(nm)	Oscillatory strength (*f*)	Major Contribution	Assignment
B3LYP	307.75	0.0064	HOMO→LUMO (90%)	n→π*
	282.20	0.0626	HOMO-3→LUMO (19%),	π→ π*
			HOMO-2→LUMO (38%),	n→π*, π→ π*
			HOMO-1→LUMO (32%)	n→ π*
	278.02	0.0836	HOMO-1→LUMO (53%)	n→ π*
	240.60	0.3769	HOMO-3→LUMO (58%),	π→ π*
			HOMO-1→LUMO+1 (15%)	n→ π*
	235.03	0.0169	HOMO-4→LUMO (97%)	n→π*
	230.55	0.0091	HOMO→LUMO+1 (96%)	n→π*
	210.38	0.3433	HOMO-2→LUMO+1 (17%),	n→π*, π→ π*
			HOMO-1→LUMO+1 (56%)	n→ π*
	206.45	0.0791	HOMO-3→LUMO+1 (19%),	π→ π*
			HOMO-2→LUMO+1 (65%)	n→π*, π→ π*

B3PW91	307.79	0.0054	HOMO→LUMO (92%)	n→π*
	283.38	0.0361	HOMO -3→LUMO (10%),	π→ π*
			HOMO -2→LUMO (63%),	n→π*, π→ π*
			HOMO -1→LUMO (18%)	n→ π*
	277.68	0.1174	HOMO -1→LUMO (67%)	n→ π*
	239.14	0.3284	HOMO -3→LUMO (63%),	π→ π*
			HOMO -1→ LUMO +1 (13%)	n→ π*
	236.73	0.0754	HOMO -4→LUMO (90%)	n→π*
	230.51	0.0082	HOMO→ LUMO +1 (97%)	n→π*
	209.97	0.2568	HOMO -2→ LUMO +1 (32%),	n→π*, π→ π*
			HOMO -1→ LUMO +1 (46%)	n→ π*
	206.59	0.1588	HOMO -3→ LUMO +1 (10%),	π→ π*
			HOMO -2→ LUMO +1 (59%)	n→π*, π→ π*
MPW1PW91	289.70	0.0042	HOMO→LUMO (69%)	n→π*
	273.88	0.1068	HOMO -3→LUMO (20%),	π→ π*
			HOMO -2→LUMO (12%),	n→π*, π→ π*
			HOMO -1→LUMO (45%),	n→ π*
			HOMO→LUMO (19%)	n→π*
	269.44	0.0616	HOMO -1→LUMO (40%)	n→ π*
	234.67	0.3879	HOMO -3→LUMO (50%)	π→ π*
	221.12	0.0025	HOMO -4→LUMO (99%)	n→π*
	216.25	0.0058	HOMO→ LUMO +1 (97%)	n→π*
	204.50	0.4503	HOMO -3→LUMO (12%),	π→ π*
			HOMO -1→ LUMO +1 (65%)	n→ π*

Table 3S List of selected excitation bands of complex **1** calculated in different functionals (B3LYP, B3PW91, MPWIPW91) in CPCM model in methanolic solution.

Functional	Wavelength λ (nm)	Oscillatory strength (*f*)	Major Contribution	Assignment[‡]
B3LYP	1058.05	0.0011	SOMO (β) → LUMO (β) (67%)	LMCT
	696.84	0.0193	SOMO -3(β) →LUMO (β) (13%),	L_1MCT
			SOMO -2(β) →LUMO (β) (23%)	LMCT
	664.29	0.0047	SOMO -8(β) → LUMO (β) (20%)	L_1MCT
			SOMO -4(β) →LUMO (β) (13%)	LMCT
	598.75	0.0137	SOMO -18(β) →LUMO (β) (13%),	IMCT
			SOMO -8 (β) →LUMO (β) (15%)	L_1MCT
	543.19	0.01	SOMO -15(β) → LUMO (β) (12%)	LMCT
			SOMO -9 (β) →LUMO (β) (13%)	LMCT
			SOMO (β) →LUMO (β) (20%)	LMCT
	441.41	0.0006	SOMO -1(β) →LUMO (β) (91%)	L_1MCT
	416.76	0.0251	SOMO -3(β) → LUMO (β)(48%)	L_1MCT
	398.63	0.0058	SOMO -7(β) →LUMO (β) (42%),	L_1MCT
			SOMO -3(β) →LUMO (β) (10%),	L_1MCT
			SOMO -2(β) →LUMO (β) (14%)	LMCT
	390.73	0.0085	SOMO -8(β) → LUMO (β)(10%)	L_1MCT
			SOMO -6 (β) → LUMO (β)(14%)	LMCT
			SOMO -2(β) →LUMO (β) (19%)	LMCT
	373.78	0.0298	SOMO -4(β) →LUMO (β) (34%),	LMCT
	362.47	0.0177	SOMO -7 (β) →LUMO (β) (23%)	L_1MCT
			SOMO -6 (β) → LUMO (β)(22%)	LMCT

	342.24	0.1845	SOMO (α) → LUMO+1(α) (16%)	ILCT
			SOMO -18(β) →LUMO (β) (14%)	IMCT
			SOMO -6(β) →LUMO (β) (13%)	LMCT
			SOMO (β) → LUMO+2(β) (15%)	ILCT
	333.83	0.005	SOMO -2(α) →LUMO+1(α) (80%)	ILCT
	317.72	0.0039	SOMO -3(β) →LUMO+1(β) (51%)	IL_1CT
	313.80	0.2182	SOMO -14(β) →LUMO (β) (11%)	LMCT
			SOMO -8(β) →LUMO (β) (31%)	L_1MCT
	295.20	0.019	SOMO -4(α) →LUMO (α) (37%),	IL_1CT
			SOMO -2(α) →LUMO (α) (31%)	LL_1CT
	291.64	0.3891	SOMO -1(α) →LUMO (α) (23%),	ILCT
			SOMO -1(β) →LUMO+1(β) (20%)	IL_1CT
	289.59	0.1553	SOMO -1(α) →LUMO+1(α) (35%),	L_1LCT
			SOMO -1(β) →LUMO+2(β) (14%)	L_1LCT
	275.27	0.0131	SOMO -5(α) →LUMO (α) (40%),	IL_1CT
			SOMO -5(β) →LUMO+1(β) (41%)	IL_1CT
	268.81	0.001	SOMO -11(β) →LUMO (β) (85%)	LMCT
	259.42	0.0273	SOMO -10(β) →LUMO (β) (62%)	L_1MCT
	258.49	0.0054	SOMO -6(α) →LUMO (α) (36%),	LL_1CT
			SOMO -6(β) →LUMO+1(β) (26%)	LL_1CT
	252.77	0.0028	SOMO -8(α) →LUMO (α) (27%),	LL_1CT
			SOMO -7(α) →LUMO (α) (10%),	IL_1CT
			SOMO -6(β) →LUMO+1(β) (18%)	LL_1CT
B3PW91	1018.92	0.0014	SOMO (β) → LUMO (β) (66%)	LMCT
	689.52	0.0174	SOMO -2(β) → LUMO (β) (38%)	LMCT
	648.38	0.0046	SOMO -8(β) → LUMO (β) (21%),	L_1MCT
			SOMO -4(β) → LUMO (β) (13%)	LMCT
	591.12	0.0125	SOMO -15(β) → LUMO (β) (17%)	LMCT
	528.30	0.0108	SOMO -15(β) → LUMO (β) (10%),	LMCT
			SOMO -9(β) → LUMO (β) (13%),	LMCT
			SOMO -3(β) → LUMO (β) (15%),	L_1MCT
			SOMO (β) → LUMO (β) (22%)	LMCT
	425.03	0.0008	SOMO -1(β) → LUMO (β) (91%)	L_1MCT
	405.87	0.0283	SOMO -3(β) → LUMO (β) (59%)	L_1MCT
	389.27	0.004	SOMO -7(β) → LUMO (β) (46%),	L_1MCT
			SOMO -2(β) → LUMO (β) (16%)	LMCT
	368.16	0.0277	SOMO -4(β) → LUMO (β) (40%)	LMCT
	356.86	0.0212	SOMO (α) → LUMO (α) (26%),	LL_1CT
			SOMO -7(β) → LUMO (β) (18%),	L_1MCT
			SOMO -5(β) → LUMO (β) (16%)	LMCT
	354.94	0.0069	SOMO (α) → LUMO (α) (69%)	LL_1CT
	338.38	0.1126	SOMO -2(α) → LUMO +1(α)	LL_1CT
			(25%),	LMCT
			SOMO -5(β) → LUMO (β) (10%),	ILCT
			SOMO (β) → LUMO +2(β) (10%)	
	335.98	0.0711	SOMO -2(α) → LUMO +1(α)	LL_1CT
			(41%)	
	317.50	0.001	SOMO -3(β) → LUMO +1(β)	IL_1CT
			(29%),	LL_1CT
			SOMO -2(β) → LUMO +1(β)	
			(27%)	
	308.91	0.273	SOMO -14(β) → LUMO (β) (15%),	LMCT
			SOMO -8(β) → LUMO (β) (39%)	L_1MCT
	295.89	0.0087	SOMO -4(α) → LUMO (α) (34%),	IL_1CT
			SOMO -3(α) → LUMO (α) (14%),	LL_1CT
			SOMO -2(α) → LUMO (α) (31%)	LL_1CT

	287.61	0.4724	SOMO -1(α) → LUMO (α) (29%), SOMO -1(β) → LUMO +1(β) (27%)	IL_1CT IL_1CT
	285.81	0.0556	SOMO -1(α) → LUMO +1(α) (55%)	L_1LCT
	271.41	0.0135	SOMO -6(α) → LUMO (α) (40%), SOMO -6(β) → LUMO +1(β) (41%)	IL_1CT IL_1CT
	264.41	0.0009	SOMO -11(β) → LUMO (β) (71%), SOMO -10(β) → LUMO (β) (10%)	LMCT L_1MCT
	257.82	0.0048	SOMO -5(α) → LUMO (α) (29%), SOMO -5(β) → LUMO +1(β) (38%)	LL_1CT LL_1CT
	255.13	0.0833	SOMO -5(α) → LUMO +1(α) (32%)	ILCT
	252.56	0.0005	SOMO -10(β) → LUMO (β) (28%)	L_1MCT
	251.97	0.0013	SOMO -10(β) → LUMO (β) (41%)	L_1MCT
MPW1PW91	953.49	0.0017	SOMO (β) → LUMO (β) (49%)	LMCT
	692.45	0.0107	SOMO -15(β) → LUMO (β) (10%), SOMO -14(β) → LUMO (β) (18%)	MMCT LMCT
	646.45	0.0032	SOMO -22(β) → LUMO (β) (12%), SOMO -8(β) → LUMO (β) (21%)	MMCT L_1MCT
	591.63	0.0061	SOMO -15(β) → LUMO (β) (20%)	MMCT
	491.47	0.0129	SOMO (β) → LUMO (β) (41%)	LMCT
	368.62	0.0016	SOMO -1(β) → LUMO (β) (90%)	L_1MCT
	359.66	0.0262	SOMO -2(β) → LUMO (β) (28%), SOMO (β) → LUMO +2(β) (11%)	LMCT ILCT
	355.84	0.0527	SOMO (α) → LUMO +1(α) (18%), SOMO -6(β) → LUMO (β) (11%), SOMO -3(β) → LUMO (β) (17%),	ILCT LMCT L_1MCT
	346.84	0.0252	SOMO -7(β) → LUMO (β) (37%), SOMO -3(β) → LUMO (β) (19%), SOMO -2(β) → LUMO (β) (14%)	L_1MCT L_1MCT LMCT
	334.89	0.0326	SOMO -2(β) → LUMO (β) (23%)	LMCT
	323.11	0.1383	SOMO -4(β) → LUMO (β) (41%)	LMCT
	312.68	0.034	SOMO -7(β) → LUMO (β) (14%), SOMO -6(β) → LUMO (β) (44%)	L_1MCT L_1MCT
	299.88	0.0018	SOMO -4(α) → LUMO (α) (12%), SOMO -3(β) → LUMO +1(β) (51%)	IL_1CT LL_1CT
	288.85	0.6984	SOMO -8(β) → LUMO (β) (32%)	L_1MCT
	278.45	0.255	SOMO -1(α) → LUMO (α) (25%), SOMO -8(β) → LUMO (β) (20%), SOMO -1(β) → LUMO +1(β) (24%)	IL_1CT L_1MCT IL_1CT
	271.21	0.0625	SOMO -9(β) → LUMO (β) (46%)	LMCT
	264.40	0.0136	SOMO -5(α) → LUMO (α) (39%), SOMO -5(β) → LUMO +1(β) (40%)	IL_1CT IL_1CT
	242.26	0.0175	SOMO -6(α) → LUMO (α) (24%), SOMO -6(β) → LUMO +1(β) (15%)	LL_1CT LL_1CT
	240.53	0.0016	SOMO -11(β) → LUMO (β) (81%)	LL_1CT
	237.78	0.0027	SOMO -8(α) → LUMO (α) (31%), SOMO -6(β) →LUMO +1(β) (23%)	LL_1CT LL_1CT
	234.53	0.0161	SOMO -7(α) → LUMO (α) (17%), SOMO -7(β) → LUMO +1(β)	IL_1CT IL_1CT

	(29%), SOMO -6(β) → LUMO +1(β) (21%)		LL_1CT

‡IMCT = Intra metal charge transfer, LMCT = Schiff base to metal charge transfer, L_1MCT = carboxylate to metal charge transfer, LL_1CT = Schiff base to carboxylate charge transfer transition, IL_1CT = Intra carboxylate charge transfer, ILCT= Intra Schiff base charge transfer, L_1LCT=carboxylate to Schiff base charge transfer.

Table 4S List of selected excitation bands of complex **2** calculated in different functionals (B3LYP, B3PW91, MPWIPW91) in CPCM model in methanolic solution.

Functional	Wavelength λ(nm)	Oscillatory strength (*f*)	Major Contribution	Assignment‡
B3LYP	1067.07	0.001	SOMO (β) →LUMO (β) (66%)	LMCT
	694.00	0.0177	SOMO -12(β) →LUMO (β) (19%),	LMCT
			SOMO -3(β) →LUMO (β) (15%)	L_1MCT
	670.03	0.0047	SOMO -8(β) →LUMO (β) (18%)	L_1MCT
	595.52	0.0132	SOMO -14(β) →LUMO (β) (10%),	LMCT
			SOMO -8(β) →LUMO (β) (15%)	L_1MCT
	547.70	0.0102	SOMO (β) →LUMO (β) (19%)	LMCT
	418.38	0.0198	SOMO -3(β) →LUMO (β) (42%),	L_1MCT
			SOMO -2(β) →LUMO (β) (17%)	LMCT
	403.06	0.0034	SOMO -7(β) →LUMO (β) (17%),	L_1MCT
			SOMO -2(β) →LUMO (β) (21%),	LMCT
			SOMO -1(β) →LUMO (β) (45%)	L_1MCT
	397.87	0.0019	SOMO -5(β) →LUMO (β) (10%),	LMCT
			SOMO -3(β) →LUMO (β) (13%),	L_1MCT
			SOMO -1(β) →LUMO (β) (33%)	L_1MCT
	391.86	0.0056	SOMO -6(β) →LUMO (β) (13%),	LMCT
			SOMO -4(β) →LUMO (β) (13%),	L_1MCT
			SOMO -2(β) →LUMO (β) (15%)	LMCT
	374.78	0.0287	SOMO -5(β) →LUMO (β) (24%)	LMCT
	366.00	0.0108	SOMO -4(β) →LUMO (β) (33%)	L_1MCT
	355.96	0.0108	SOMO -7(β) →LUMO (β) (37%),	L_1MCT
			SOMO -5(β) →LUMO (β) (12%),	LMCT
			SOMO -4(β) →LUMO (β) (26%)	L_1MCT
	341.90	0.1582	SOMO (α) →LUMO (α) (17%),	ILCT
			SOMO -17(β) →LUMO (β) (10%),	LMCT
			SOMO -6(β) →LUMO (β) (12%),	LMCT
			SOMO (β) →LUMO +1(β) (16%)	ILCT
	333.29	0.0034	SOMO -1(α) →LUMO (α) (87%)	ILCT
	312.48	0.1074	SOMO -13(β) →LUMO (β) (13%),	LMCT
			SOMO -8(β) →LUMO (β) (40%)	L_1MCT
	305.61	0.0021	SOMO (α) →LUMO +1(α) (85%)	LL_1CT
	294.22	0.0439	SOMO -11(β) →LUMO (β) (14%),	LMCT
			SOMO -9(β) →LUMO (β) (20%),	LMCT
			SOMO -5(β) →LUMO +1(β) (12%),	ILCT
			SOMO-2(β) →LUMO +1(β) (18%)	ILCT
	282.59	0.0002	SOMO -1(α) →LUMO +1(α) (22%),	LL_1CT
			SOMO -3(β) →LUMO +2(β) (48%)	IL_1CT
	269.61	0.001	SOMO -4(α) →LUMO (α) (15%),	L_1LCT
			SOMO -2(α) →LUMO (α) (14%),	L_1LCT
			SOMO -10(β) →LUMO (β) (46%)	LMCT
	269.38	0.0009	SOMO -10(β) →LUMO (β) (41%)	LMCT
	253.15	0.0213	SOMO -4(β) →LUMO +2(β) (20%)	IL_1CT
	248.14	0.0042	SOMO -2(β) → LUMO +2(β) (23%)	LL_1CT
	244.41	0.0207	SOMO -7(β) → LUMO +1(β) (49%)	L_1LCT

B3PW91	1028.56	0.0013	SOMO (β) →LUMO (β) (65%)	LMCT
	689.21	0.0156	SOMO -12(β) → LUMO (β) (17%),	LMCT
			SOMO -2(β) → LUMO (β) (33%)	L_1MCT
	651.61	0.0044	SOMO -8(β) →LUMO (β) (19%)	L_1MCT
	589.30	0.012	SOMO -8(β) → LUMO (β) (15%)	L_1MCT
	532.16	0.0111	SOMO (β) → LUMO (β) (22%)	LMCT
	474.79	0.0003	SOMO (β) → LUMO +1(β) (47%)	ILCT
	407.22	0.0215	SOMO -3(β) →LUMO (β) (53%)	L_1MCT
	390.90	0.0044	SOMO -7(β) →LUMO (β) (29%),	L_1MCT
			SOMO -1(β) →LUMO (β) (11%)	L_1MCT
	386.43	0.0031	SOMO -6(β) → LUMO (β) (14%),	LMCT
			SOMO -3(β) → LUMO (β) (10%),	L_1MCT
			SOMO -1(β) → LUMO (β) (39%)	L_1MCT
	369.08	0.0282	SOMO -6(β) → LUMO (β) (19%),	LMCT
			SOMO -5(β) → LUMO (β) (23%),	LMCT
			SOMO -4(β) → LUMO (β) (13%)	L_1MCT
	358.13	0.0201	SOMO -6(β) → LUMO (β) (21%)	LMCT
	345.96	0.0157	SOMO -7(β) → LUMO (β) (31%),	L_1MCT
			SOMO -4(β) → LUMO (β) (30%)	L_1MCT
	337.56	0.1081	SOMO -1(α) → LUMO (α) (22%),	ILCT
			SOMO (α) → LUMO (α) (10%),	ILCT
			SOMO -6(β) → LUMO (β) (11%),	LMCT
			SOMO (β) → LUMO +1(β) (11%)	ILCT
	335.40	0.0412	SOMO -1(α) → LUMO (α) (66%)	ILCT
	307.42	0.1163	SOMO -13(β) →LUMO (β) (16%),	LMCT
			SOMO -8(β) → LUMO (β) (43%)	L_1MCT
	303.41	0.0016	SOMO (α) → LUMO +1(α) (79%),	LL_1CT
			SOMO (β) → LUMO +2(β) (12%)	LL_1CT
	286.25	0.0308	SOMO -11(β) → LUMO (β) (19%),	LMCT
			SOMO -9(β) → LUMO (β) (34%)	LMCT
	281.42	0.0002	SOMO -1(α) → LUMO +1(α) (23%),	LL_1CT
			SOMO -3(β) →LUMO +2(β) (18%),	IL_1CT
			SOMO -2(β) → LUMO +2(β) (34%)	IL_1CT
	265.15	0.0011	SOMO -10(β) → LUMO (β) (83%)	LMCT
	263.76	0.0356	SOMO -3(β) → LUMO +1(β)(19%),	ILCT
			SOMO -1(β) → LUMO +1(β) (50%)	L_1LCT
	261.52	0.0027	SOMO -1(α) →LUMO +1(α) (40%)	LL_1CT
	255.74	0.1082	SOMO -6(α) →LUMO (α) (23%)	ILCT
	249.24	0.0067	SOMO -5(α) → LUMO +1(α) (16%)	L_1LCT
	246.97	0.0422	SOMO -12(β) → LUMO (β) (28%),	LMCT
			SOMO -11(β) →LUMO (β) (13%)	LMCT
	243.80	0.0124	SOMO -18(β) → LUMO (β) (11%),	L_1MCT
			SOMO -13(β) → LUMO (β) (32%)	LMCT
MPW1PW91	960.66	0.0016	SOMO (β) → LUMO (β) (49%)	LMCT
	691.29	0.0096	SOMO -13(β) → LUMO (β) (18%)	LMCT
	649.39	0.0028	SOMO -8(β) → LUMO (β) (19%)	L_1MCT
	589.72	0.0056	SOMO -27(β) → LUMO (β) (31%),	MMCT
			SOMO -15(β) → LUMO (β) (18%)	LMCT
	493.74	0.0133	SOMO (β) →LUMO (β) (41%)	LMCT
	359.97	0.0181	SOMO -3(β) → LUMO (β) (20%),	L_1MCT

		SOMO -2(β) → LUMO (β) (32%)	LMCT
356.35	0.0489	SOMO (α) → LUMO (α) (18%),	ILCT
		SOMO -7(β) →LUMO (β) (10%),	L_1MCT
		SOMO -3(β) →LUMO (β) (18%),	L_1MCT
		SOMO (β) → LUMO +1(β) (18%)	ILCT
346.74	0.0173	SOMO -7(β) →LUMO (β) (33%),	L_1MCT
		SOMO -4(β) → LUMO (β) (15%),	L_1MCT
		SOMO -2(β) → LUMO (β) (15%)	LMCT
337.88	0.0005	SOMO -5(β) → LUMO (β) (10%),	LMCT
		SOMO -1(β) → LUMO (β) (76%)	L_1MCT
334.94	0.0303	SOMO -2(β) → LUMO (β) (24%)	LMCT
323.09	0.1177	SOMO -5(β) → LUMO (β) (37%)	LMCT
313.54	0.033	SOMO -6(β) → LUMO (β) (47%),	LMCT
		SOMO -4(β) → LUMO (β) (10%)	L_1MCT
305.15	0.0031	SOMO -4(β) → LUMO (β) (54%)	L_1MCT
287.49	0.0035	SOMO (α) → LUMO +1(α) (46%),	LL_1CT
		SOMO (β) → LUMO +2(β) (35%)	LL_1CT
283.92	0.1007	SOMO -8(β) → LUMO (β) (45%)	L_1MCT
271.94	0.0349	SOMO -11(β) → LUMO (β) (15%),	LMCT
		SOMO -9(β) → LUMO (β) (47%)	LMCT
269.58	0.0004	SOMO -5(α) → LUMO +1(α) (11%),	IL_1CT
		SOMO -1(α) → LUMO +1(α) (16%),	LL_1CT
		SOMO -3(β) → LUMO +2(β) (44%)	IL_1CT
250.21	0.0535	SOMO -2(α) → LUMO (α) (59%)	L_1 LCT
245.10	0.0092	SOMO -4(β) → LUMO +2(β) (30%)	IL_1CT
240.84	0.0025	SOMO -10(β) → LUMO (β) (85%)	LMCT
233.16	0.3274	SOMO -2(α) → LUMO +1(α) (24%),	IL_1CT
		SOMO -2(β) → LUMO +2(β) (27%),	LL_1CT

[‡]IMCT = Intra metal charge transfer, LMCT = Schiff base to metal charge transfer, L_1MCT = carboxylate to metal charge transfer, LL_1CT = Schiff base to carboxylate charge transfer transition, IL_1CT = Intra carboxylate charge transfer, ILCT= Intra Schiff base charge transfer, L_1LCT=carboxylate to Schiff base charge transfer.

Table 5S Experimental and calculated[§] (using B3LYP, B3PW91, MPW1PW91 functionals) UV-vis spectral bands of complexes **1** and **2**.

Complex	Exp	Calcd		
		B3LYP	B3PW91	MPW1PW91
	222	-	-	-
1	242	-	-	-
	269	268.81	271.41	271.21
	365	362.47	368.16	368.62
	204	-	-	-
2	236	-	-	-
	270	269.61	265.15	269.58
	365	366.00	369.08	359.97

[§]Using conductor-like polarizable continuum model (CPCM) in methanol; basis set, LanL2DZ.

Table 6S Experimental and calculated[j] (using B3LYP, B3PW91, MPW1PW91functionals) electronic spectral bands of HL.

Exp (nm)	Calcd (nm)		
	B3LYP	B3PW91	MPW1PW91
400	-	-	-
316	-	-	-
278	278.02	277.68	273.88
254	240.60	239.14	234.67
214	210.38	209.97	216.25

[j]Basis set, 6-31G (d-p); using conductor-like polarizable continuum model (CPCM) in methanol.

Table 7S List of theoretically [basis set LanL2DZ, CPCM model in methanol] possible electronic transitions for model compound [Cu(L)(NO_3)].

Excitation	Wavelength λ(nm)	Oscillatory strength (*f*)	Major Contribution	Assignment ‡
1	1170.75	0.0005	SOMO(β) →LUMO(β)	LMCT
2	661.13	0.011	SOMO -13(β) →LUMO (β)(17%),	LMCT
			SOMO -3(β) →LUMO (β)(12%),	LMCT
			SOMO -1(β) →LUMO (β)(13%)	LMCT
3	630.66	0.0036	SOMO -5(β) →LUMO (β)(21%)	L_1MCT
4	591.94	0.0257	SOMO -9(β) →LUMO (β)(10%),	L_1MCT
			SOMO -3(β) →LUMO (β)(13%),	LMCT
			SOMO (β) →LUMO (β)(12%)	LMCT
5	544.40	0.0039	SOMO -23(β) →LUMO (β)(17%),	IMCT
			SOMO -14(β) →LUMO (β)(23%)	LMCT
7	433.73	0.0029	SOMO -1(β) →LUMO (β)(63%)	LMCT
9	405.57	0.0004	SOMO -3(β) →LUMO (β)(24%),	LMCT
			SOMO -2(β) →LUMO (β)(73%)	LMCT
13	384.85	0.0434	SOMO (α) → LUMO +1(α) (12%),	ILCT
			SOMO -3(β) →LUMO (β)(16%),	LMCT
			SOMO (β) → LUMO +2(β)(12%)	ILCT
15	358.09	0.0594	SOMO -4(β) →LUMO (β)(38%)	L_1MCT
16	349.101	0.0005	SOMO -4(α) →LUMO (α) (12%),	L_1MCT
			SOMO -1(α) →LUMO (α) (23%),	LMCT
			SOMO -4(β) → LUMO +1(β)(49%)	IL_1CT
17	340.00	0.136	SOMO (α) → LUMO +1(α) (25%),	ILCT
			SOMO (β) → LUMO +2(β)(23%)	ILCT
19	324.12	0.0003	SOMO -1(α) →LUMO +1(α) (86%)	ILCT
20	318.24	0.0127	SOMO -6(β) →LUMO (β)(48%)	L_1MCT
22	305.12	0.0004	SOMO -1(α) →LUMO (α) (51%)	LMCT
23	298.55	0.0108	SOMO -7(β) →LUMO (β)(59%),	L_1MCT
			SOMO -5(β) →LUMO (β)(17%)	L_1MCT
25	289.72	0.016	SOMO -9(β) →LUMO (β)(38%),	L_1MCT
			SOMO -1(β) → LUMO +1(β)(12%)	LL_1CT

28	285.47	0.0066	SOMO -8(β) →LUMO (β)(77%)	LMCT
31	275.06	0.0281	SOMO -12(β) →LUMO (β)(13%),	LMCT
			SOMO -10(β) →LUMO (β)(46%)	L_1MCT
32	274.57	0.0033	SOMO -3(α) →LUMO (α) (45%),	LMCT
			SOMO -3(β) → LUMO +1(β)(30%)	LL_1CT
34	271.48	0.0942	SOMO -10(β) →LUMO (β)(17%)	L_1MCT
35	266.52	0.0077	SOMO -12(β) →LUMO (β)(12%),	LMCT
			SOMO -11(β) →LUMO (β)(51%)	LMCT
37	259.00	0.0002	SOMO -10(α) →LUMO (α) (17%),	L_1MCT
			SOMO -5(α) →LUMO (α) (33%),	LMCT
			SOMO -10(β) → LUMO +1(β)(23%)	IL_1CT
38	258.52	0.0016	SOMO -13(β) →LUMO (β)(14%),	LMCT
			SOMO -12(β) →LUMO (β)(25%)	LMCT
42	251.85	0.0884	SOMO -3(α) → LUMO +1(α) (33%),	ILCT
			SOMO -2(β) → LUMO +2(β)(36%)	ILCT
47	238.76	0.0045	SOMO -15(β) →LUMO (β)(36%)	LMCT

‡IMCT = Intra metal charge transfer, LMCT = Schiff base to metal charge transfer, L_1MCT = Nitrate to metal charge transfer, LL_1CT = Schiff base to nitrate charge transfer transition, IL_1CT = Intra nitrate charge transfer, ILCT= Intra Schiff base charge transfer, L_1LCT=Nitrate to Schiff base charge transfer.

Table 8S. Selected MOs along with their energies and compositions of complex HL.

MOs	Energy (eV)	% of composition			
		Aromatic ring	Hydroxyl	Imine	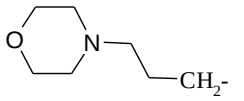
LUMO+5	2.65	88	1	2	9
LUMO+4	2.50	5	0	3	92
LUMO+3	2.03	17	67	1	16
LUMO+2	1.36	53	1	42	4
LUMO+1	0.05	94	4	2	0
LUMO	-1.13	57	1	39	3
HOMO	-5.79	1	0	3	96
HOMO -1	-6.13	17	69	10	4
HOMO -2	-6.70	26	2	57	15
HOMO -3	-6.78	66	1	25	8
HOMO -4	-6.88	1	0	0	99
HOMO -5	-8.23	3	0	3	94

Table 9S Calculated energies of optimized geometries and other physical parameters for complexes **1**, **2** and **HL**, using B3LYP, B3PW91 and MPW1PW91 functionals. [In methanol using CPCM model, basis set LanL2DZ for 1 and 2, 6-31G (d-p) for HL].

Compounds	Parameters	Functional		
		B3LYP	B3PW91	MPW1PW91
1	Charge	0	0	0
	Spin	Doublet	Doublet	Doublet
	Energy (eV)	-40777.75	-40765.53	-40769.81
	Dipole Moment	9.0218	9.0843	9.1042
	Point Group	C1	C1	C1
2	Charge	0	0	0
	Spin	Doublet	Doublet	Doublet

	Energy (eV)	-39741.54	-39729.79	-39733.91
	Dipole Moment	8.6111	8.7055	8.6866
	Point Group	C1	C1	C1
HL	Charge	0	0	0
	Spin	Singlet	Singlet	Singlet
	Energy (eV)	-21918.23	-21910.03	-21913.13
	Dipole Moment	2.6295	2.6259	2.6458
	Point Group	C1	C1	C1

Table 10S Calculated energy of optimized geometry and other physical parameters model compound using B3LYP functional. [In methanol using CPCM model, basis set LanL2DZ].

Charge	0
Spin	Doublet
Energy (eV)	-34864.93
Dipole moment (D)	14.5311
Point group	C1

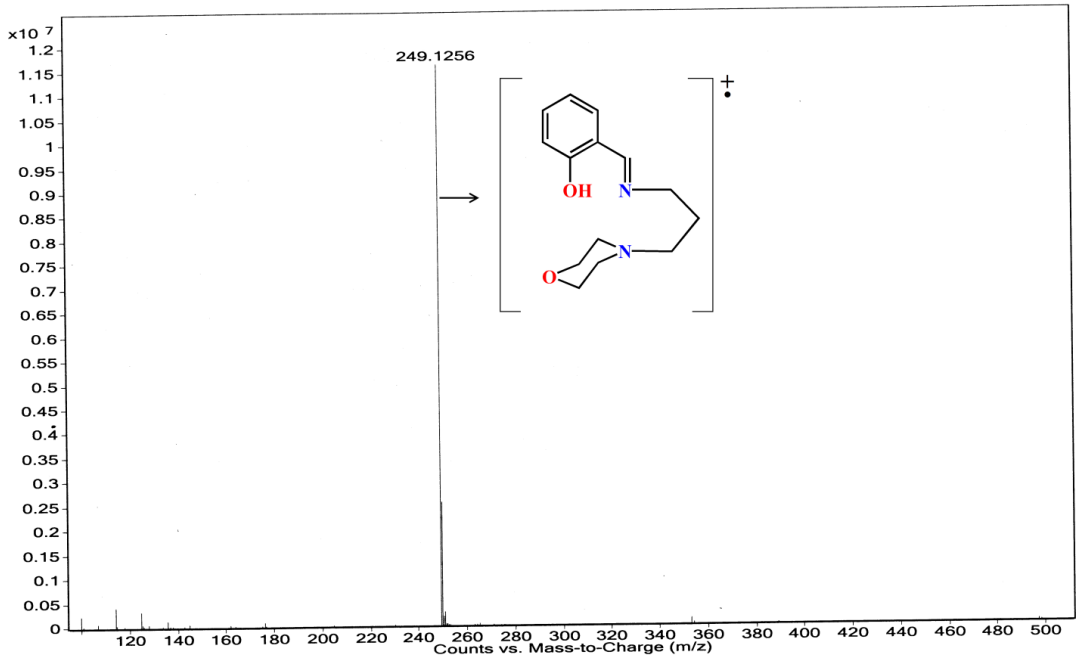

Fig.1S. ESI mass spectra of HL recorded in methanol.

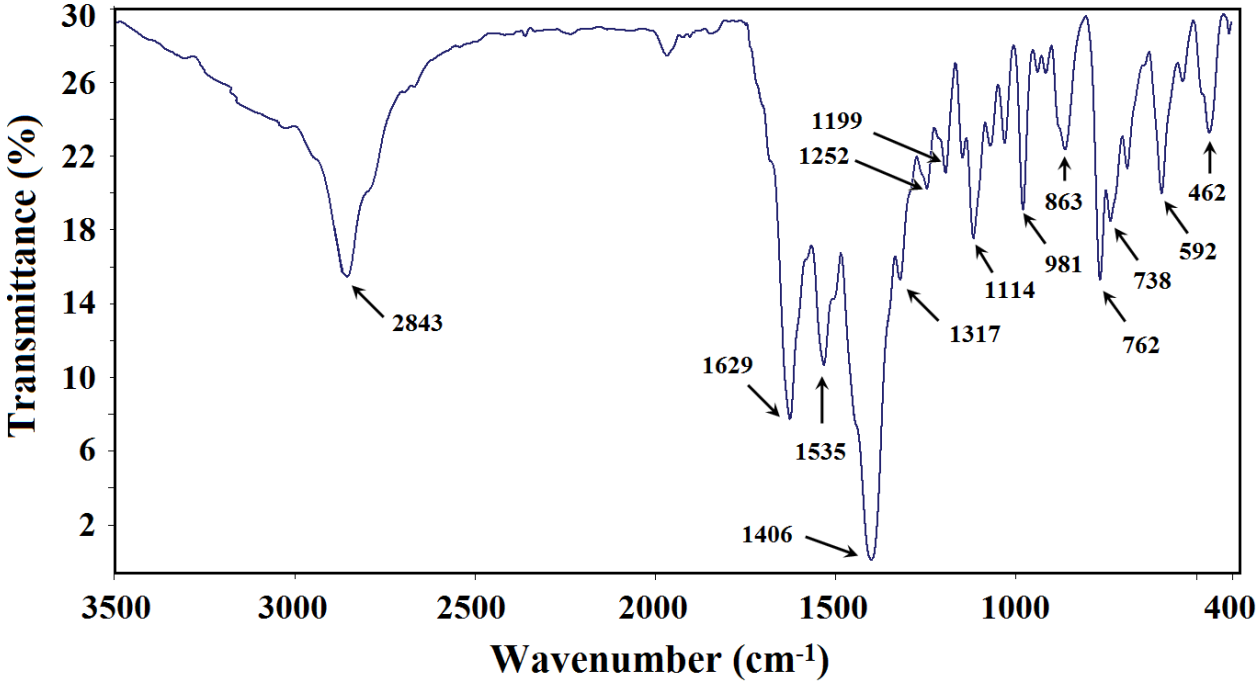

Fig.2S. FT-IR spectrum of complex **1**.

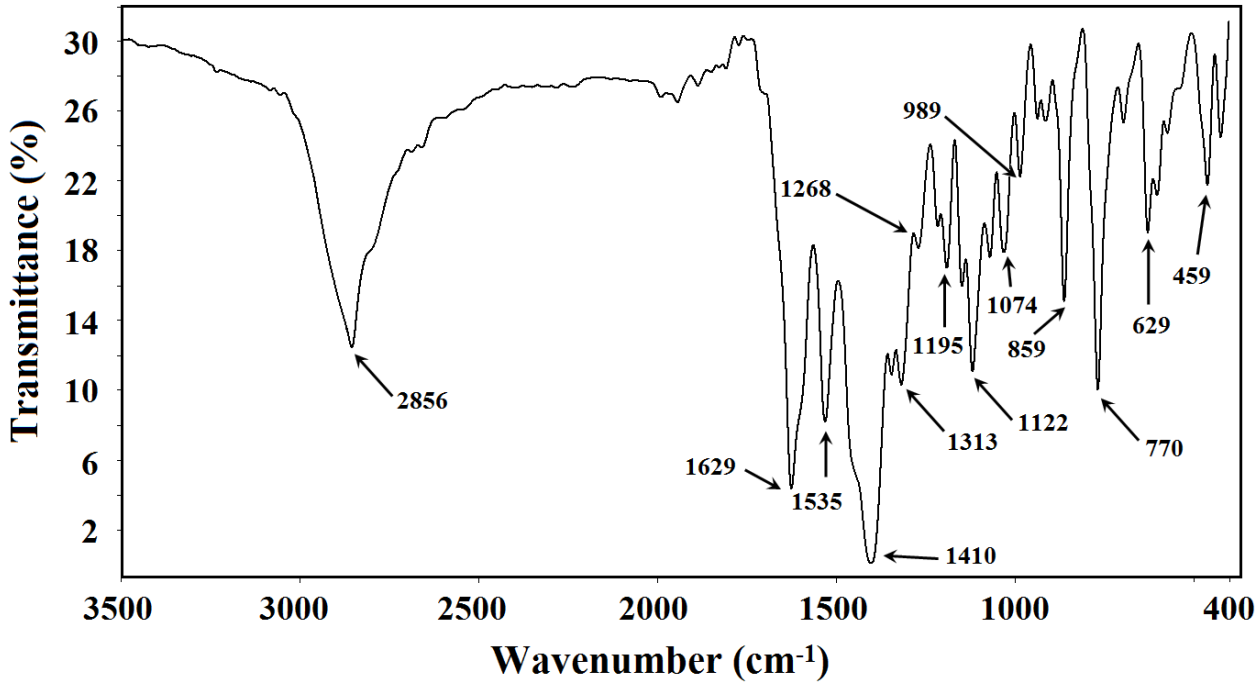

Fig.3S. FT-IR spectrum of complex **2**.

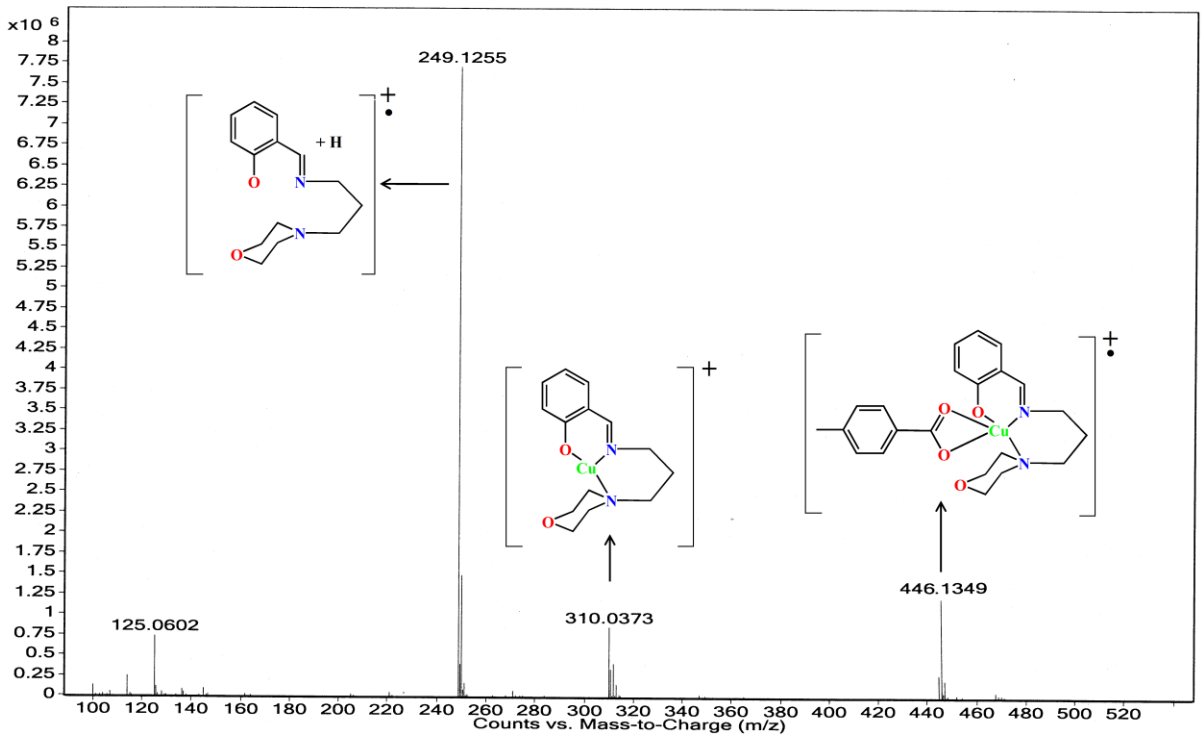

Fig.4S. ESI mass spectra of complex **2** recorded in methanol.

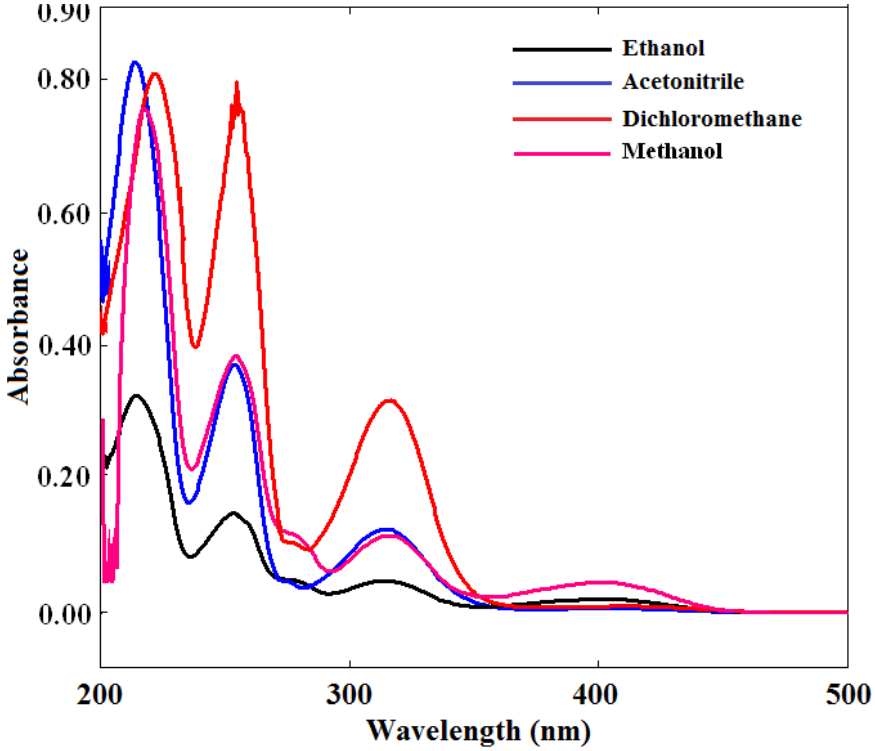

Fig.5S. Electronic absorption spectra of **HL** recorded in acetonitrile (blue line), methanol (pink line), ethanol (black line) and dichloromethane (red line).

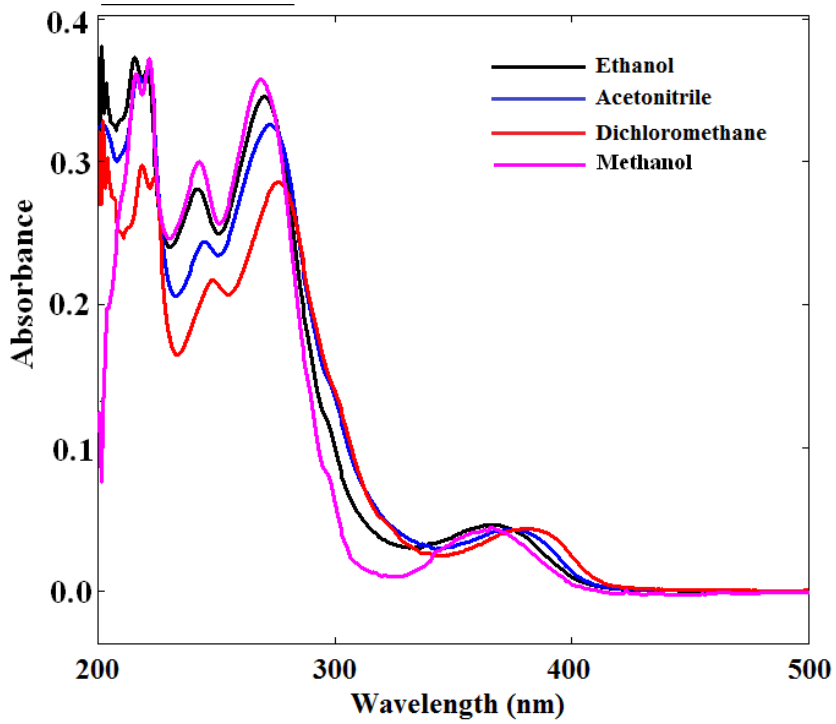

Fig.6S. Electronic absorption spectra of complex **1** recorded in acetonitrile (blue line), methanol (pink line), ethanol (black line) and dichloromethane (red line).

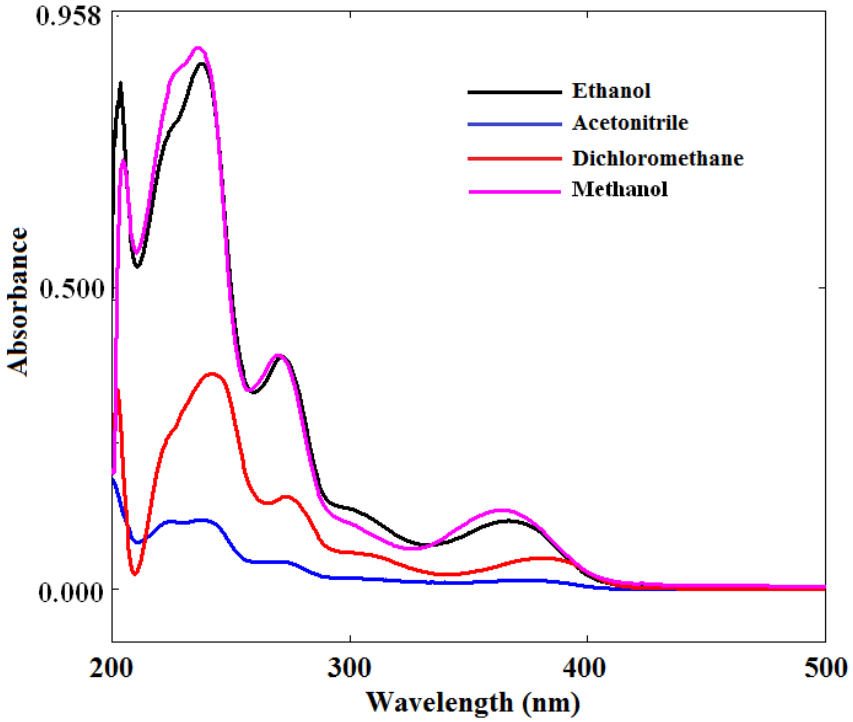

Fig.7S. Electronic absorption spectra of complex **2** recorded in acetonitrile (blue line), methanol (pink line), ethanol (black line) and dichloromethane (red line).

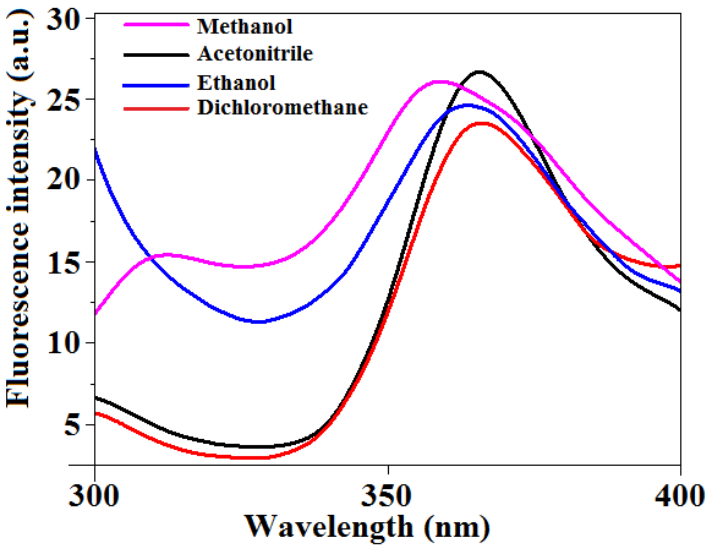

Fig.8S. Fluorescence spectra of **HL** recorded in acetonitrile (black line), methanol (pink line), ethanol (blue line) and dichloromethane (red line) [λ_{ex} = 254 nm, for all solvents].

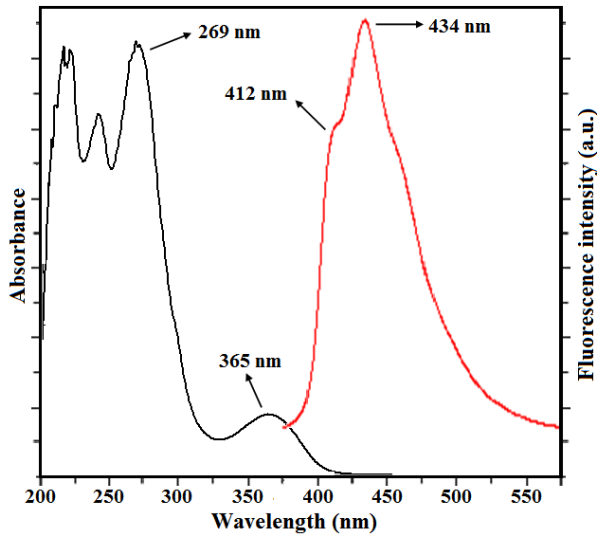

Fig.9S. Absorption (left) and fluorescence (right) spectra of complex **1**.

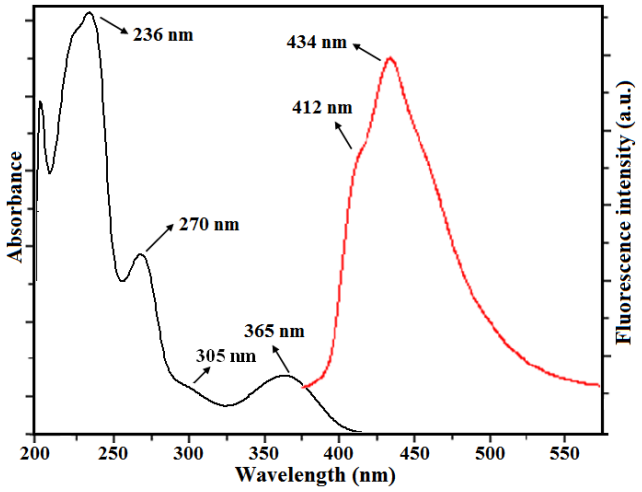

Fig.10S. Absorption (left) and fluorescence (right) spectra of complex **2**.

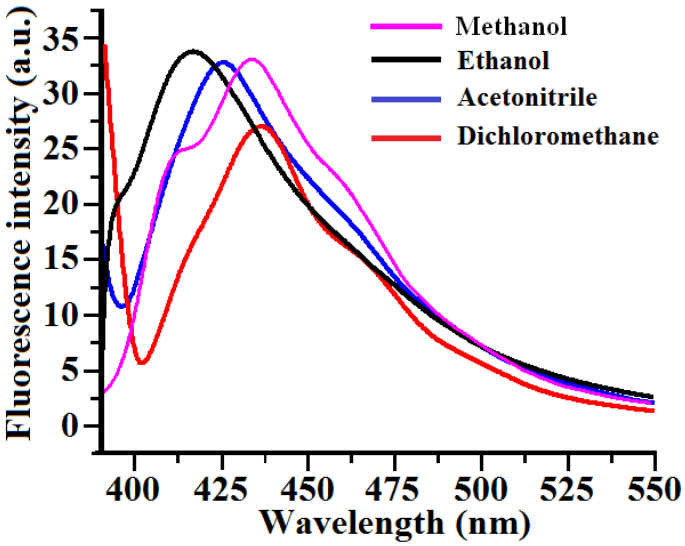

Fig.11S. Fluorescence spectra of complex **1** recorded in acetonitrile (blue line), methanol (pink line), ethanol (black line) and dichloromethane (red line).

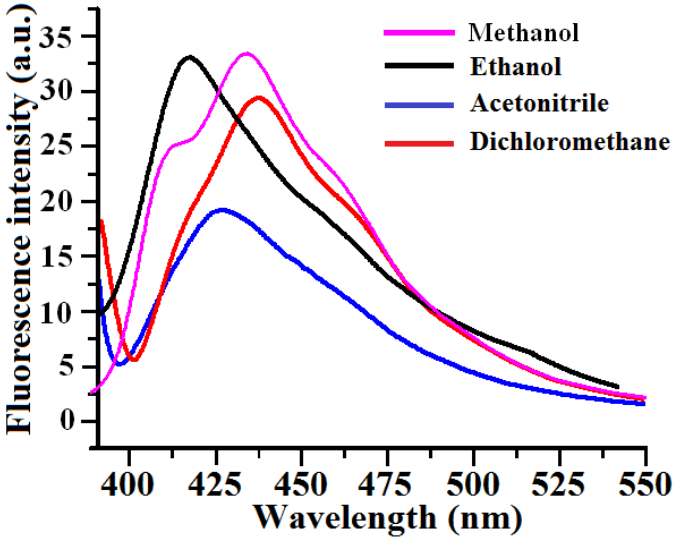

Fig.12S. Fluorescence spectra of complex **2** recorded in acetonitrile (blue line), methanol (pink line), ethanol (black line) and dichloromethane (red line).

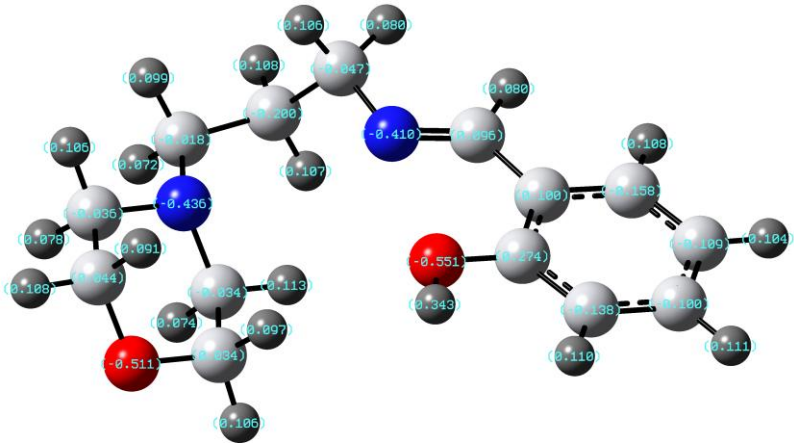

Fig.13S. Optimized structure of HL with Mulliken charge distribution (basis set, 6-31G (d-p)).

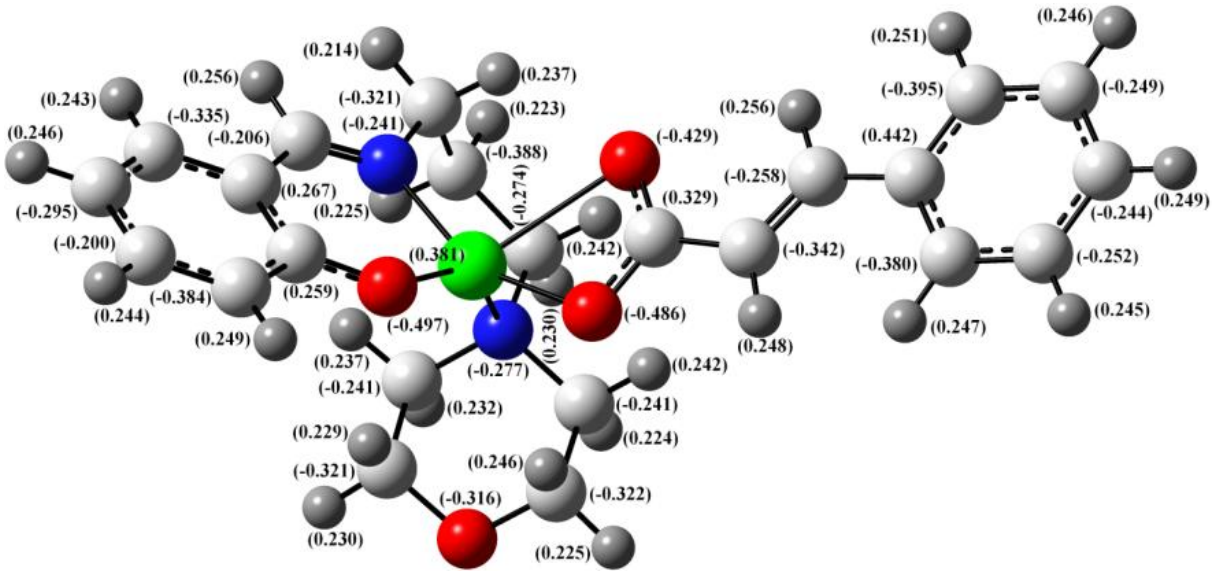

Fig.14S. Optimized structure of complex **1** with Mulliken charge distribution (basis set, LanL2DZ).

.

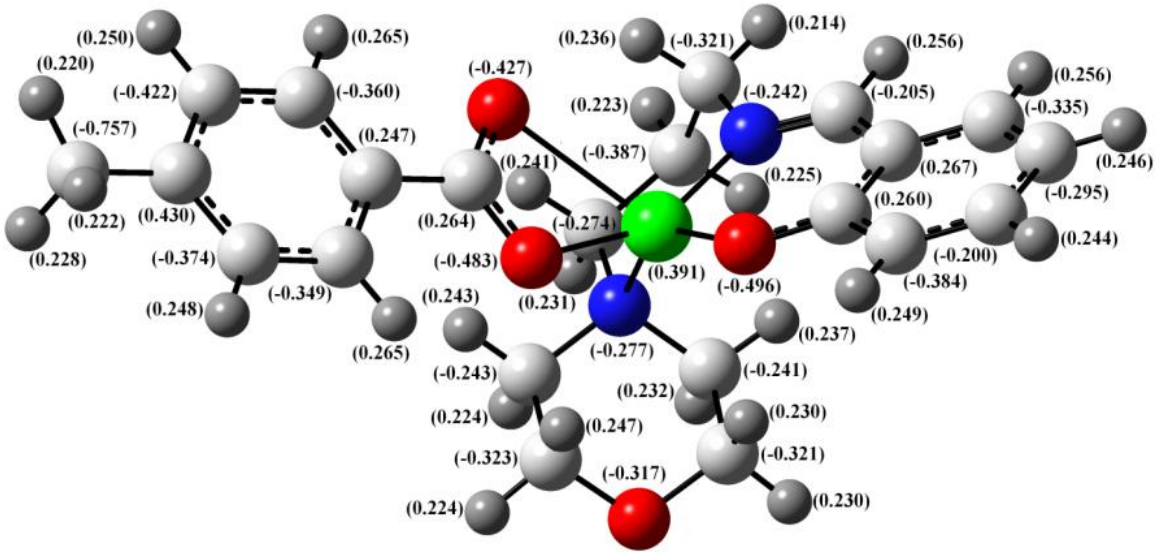

Fig.15S. Optimized structure of complex **2** with Mulliken charge distribution (basis set, LanL2DZ).

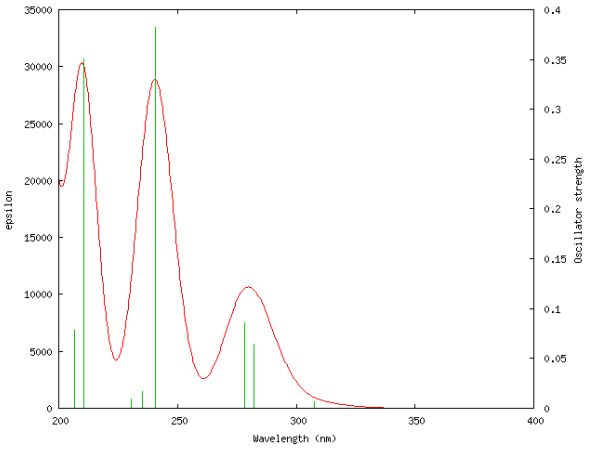

Fig. 16S. Calculated electronic absorption spectrum of **HL** [using conductor-like polarizable continuum model (CPCM) in ethanol; basis set, 6-31G(d-p)].

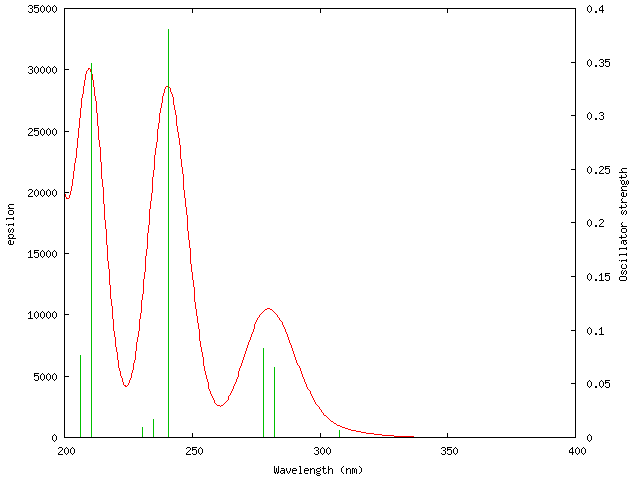

Fig. 17S. Calculated electronic absorption spectrum of **HL** [using conductor-like polarizable continuum model (CPCM) in acetonitrile; basis set, 6-31G(d-p)].

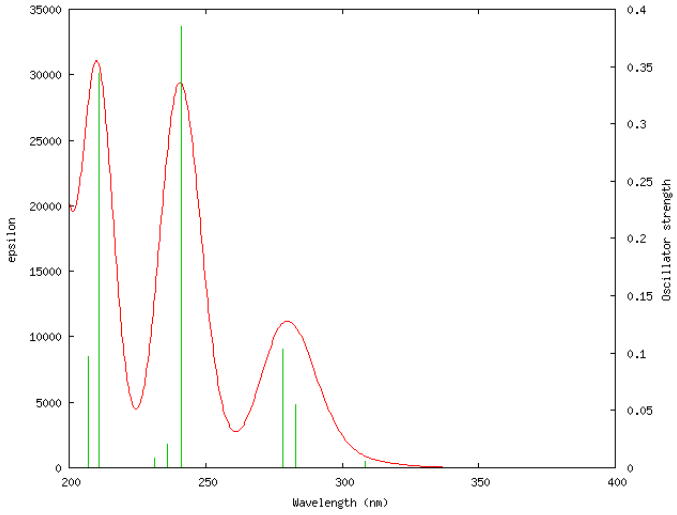

Fig. 18S. Calculated electronic absorption spectrum of **HL** [using conductor-like polarizable continuum model (CPCM) in dichloromethane; basis set, 6-31G(d-p)].

MOs	**B3LYP**	**B3PW91**	**MPW1PW91**
SOMO (α)	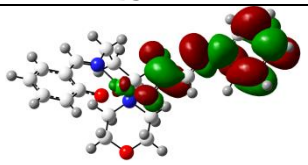 E = -5.9 eV, composition: L 96%, L_1 1%, Cu 3%	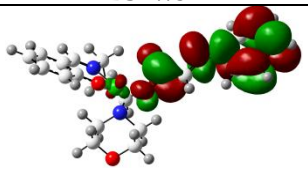 E = -5.98 eV, composition: L 96%, L_1 1%,Cu 3%	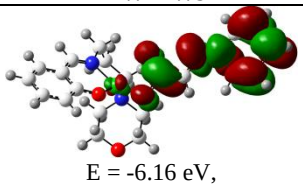 E = -6.16 eV, composition: L 97%,L_1 1%,Cu 2%

SOMO (β)	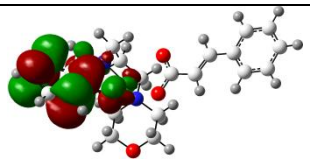 E = -5.84 eV, composition: L 95%,L_1 1%,Cu 4%	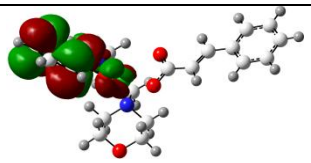 E = -5.92 eV, composition: L 95%,L_1 1%,Cu 4%	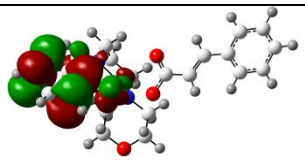 E = -6.1 eV, composition: L 95%,L_1 1%,Cu 4%
LUMO (α)	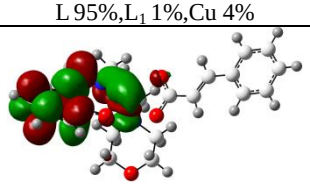 E = -2.0 eV, composition: L 1%,L_1 98%,Cu 1%	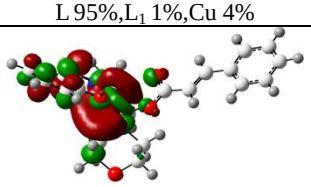 E = -2.05 eV, composition: L 1%,L_1 98%,Cu 1%	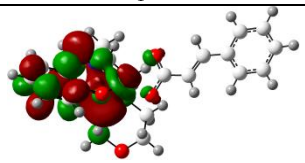 E = -1.88 eV, composition: L 1%,L_1 98%,Cu 1%
LUMO (β)	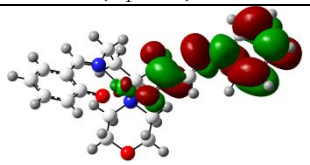 E = -3.2 eV, composition: L 32%,L_1 7%,Cu 61%	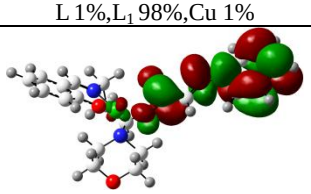 E = -3.2 eV, composition: L 33%,L_1 7%,Cu 60%	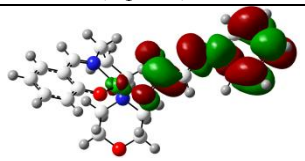 E = -2.8 eV, composition: L 29%,L_1 7%,Cu 64%

Fig. 19S. Surface plot of frontier orbitals along with their energies and compositions of complex **1** using B3LYP, B3PW91 and MPW1PW91 functionals.

MOs	**B3LYP**	**B3PW91**	**MPW1PW91**
SOMO (α)	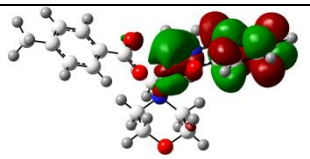 E = -5.9 eV, composition: L 97%,L_1 1%,Cu 2%	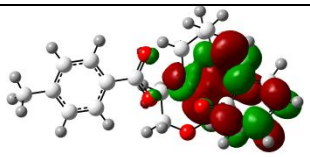 E = -5.98 eV, composition: L 96%, L_1 1%, Cu 3%	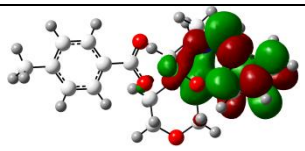 E = -6.16 eV, composition: L 66%,L_1 22%,Cu 12%
SOMO (β)	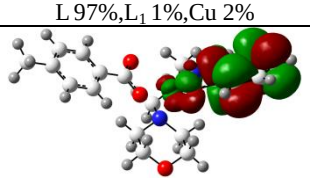 E = -5.85 eV, composition: L 95%,L_1 1%,Cu 4%	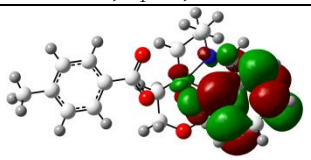 E = -5.92 eV, composition: L 95%, L_1 1%,Cu 4%	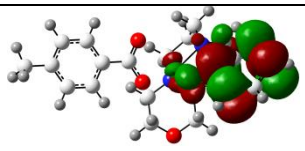 E = -6.11 eV, composition: L 95%,L_1 1%,Cu 4%
LUMO (α)	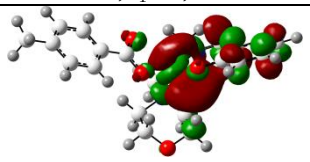 E = -1.88 eV, composition: L 99%,L_1 0%,Cu 1%	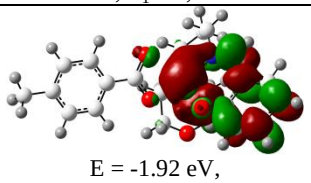 E = -1.92 eV, composition: L 99%,L_1 0%,Cu 1%	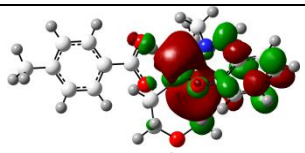 E = -1.73 eV, composition: L 99%,L_1 0%,Cu 1%

LUMO (β)	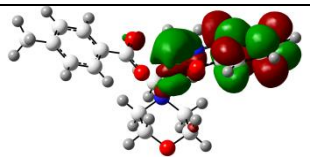 E = -3.22 eV, composition: L 32%,L_1 7%,Cu 61%	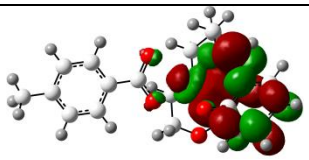 E = -3.21 eV, composition: L 32%,L_1 7%,Cu 61%	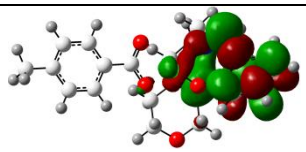 E = -2.81 eV, composition: L 29%,L_1 7%,Cu 64%

Fig. 20S. Surface plot of frontier orbitals along with their energies and compositions of complex **2** using B3LYP, B3PW91 and MPW1PW91 functionals.

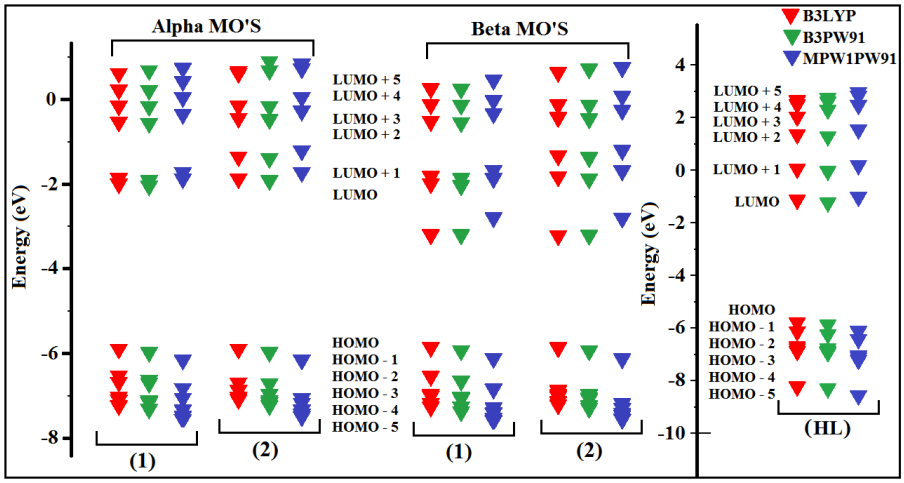

Fig.21S. Calculated molecular orbital energy level diagram of **1, 2** and HL using B3LYP, B3PW91 and MPW1PW91 functionals. [red, B3LYP; green B3PW91; blue, MPW1PW91].

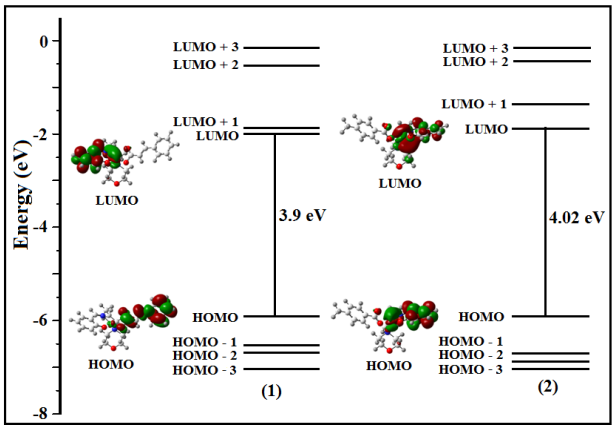

Fig.22S. Calculated α molecular orbital energy level diagram of **1** and **2** [B3LYP functional; basis set LanL2DZ; using conductor-like polarizable continuum model (CPCM) in methanol].

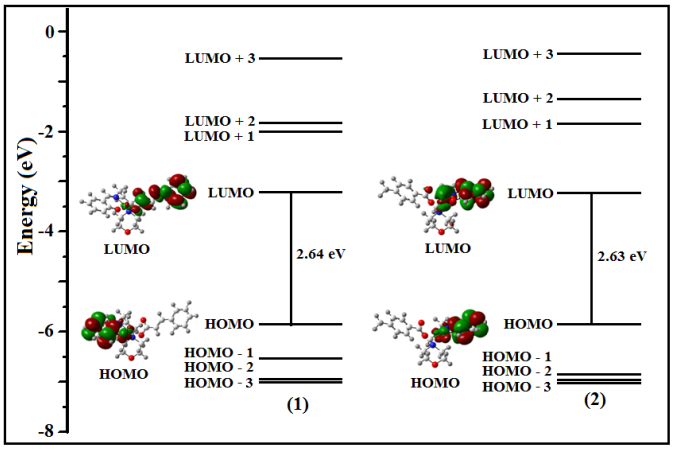

Fig.23S. Calculated β molecular orbital energy level diagram of **1** and **2** [B3LYP functional; basis set LanL2DZ, using conductor-like polarizable continuum model (CPCM) in methanol].

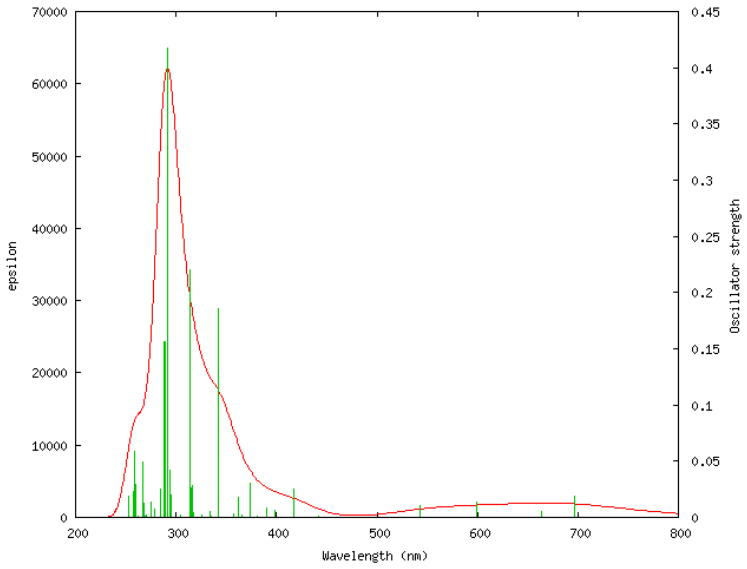

Fig. 24S. Calculated electronic absorption spectrum of **1** [using conductor-like polarizable continuum model (CPCM) in ethanol; basis set, LanL2DZ].

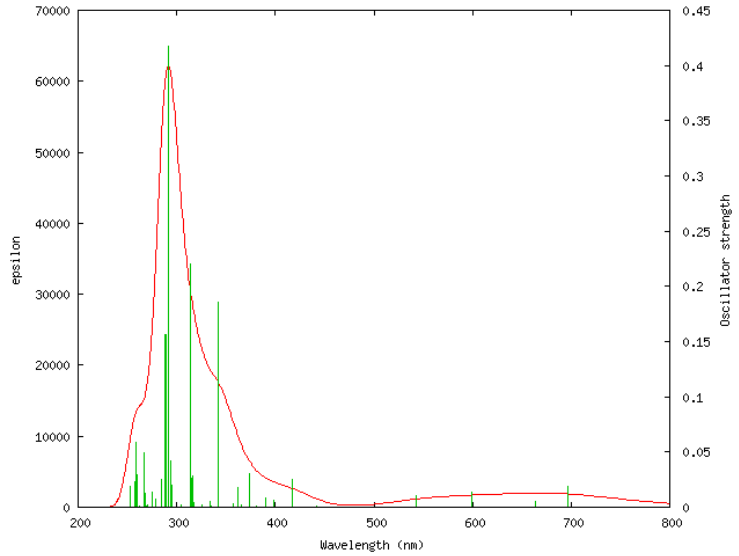

Fig. 25S. Calculated electronic absorption spectrum of **1** [using conductor-like polarizable continuum model (CPCM) in acetonitrile; basis set, LanL2DZ].

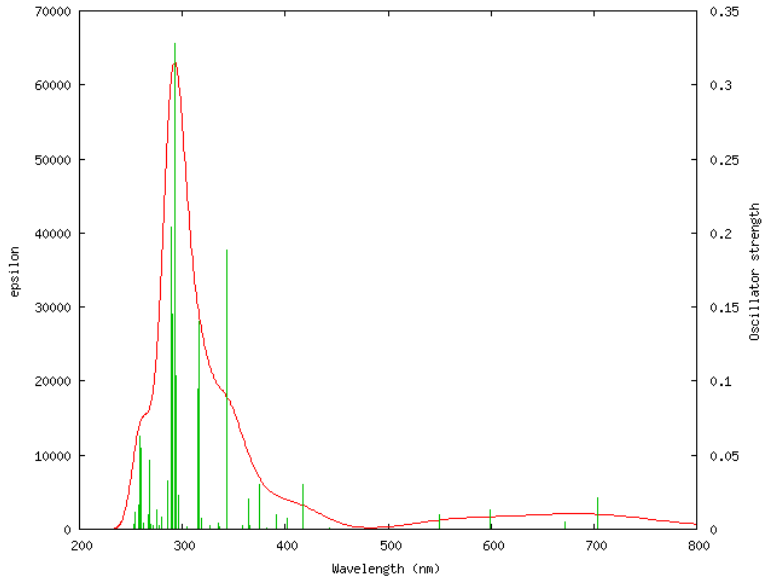

Fig. 26S. Calculated electronic absorption spectrum of **1** [using conductor-like polarizable continuum model (CPCM) in dichloromethane; basis set, LanL2DZ].

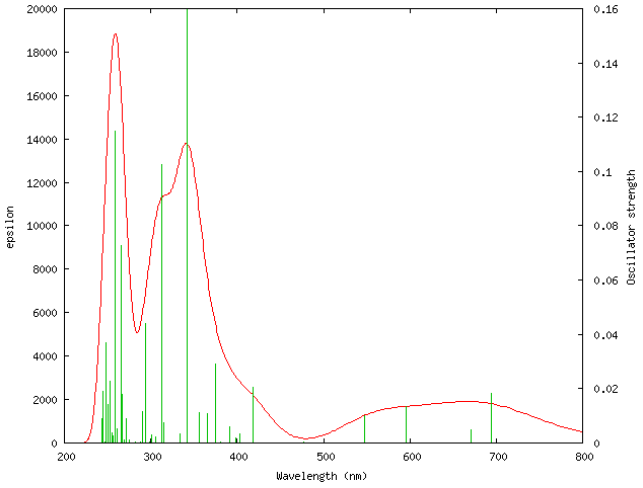

Fig. 27S. Calculated electronic absorption spectrum of **2** [using conductor-like polarizable continuum model (CPCM) in ethanol; basis set, LanL2DZ].

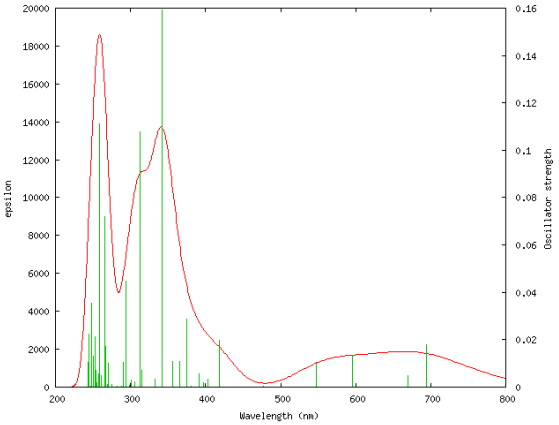

Fig. 28S. Calculated electronic absorption spectrum of **2** [using conductor-like polarizable continuum model (CPCM) in acetonitrile; basis set, LanL2DZ].

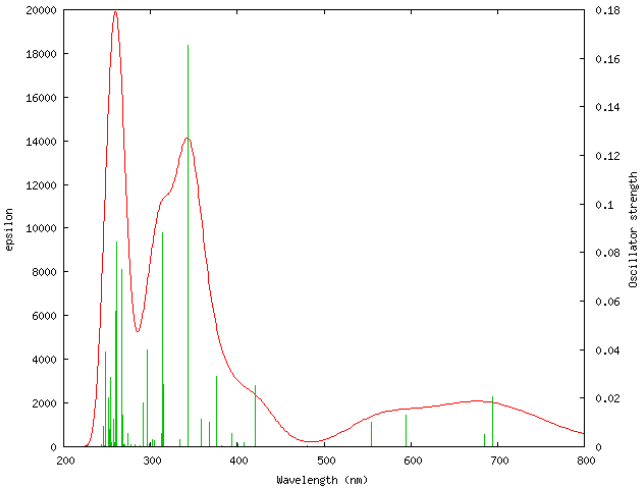

Fig. 29S. Calculated electronic absorption spectrum of **2** [using conductor-like polarizable continuum model (CPCM) in dichloromethane; basis set, LanL2DZ].

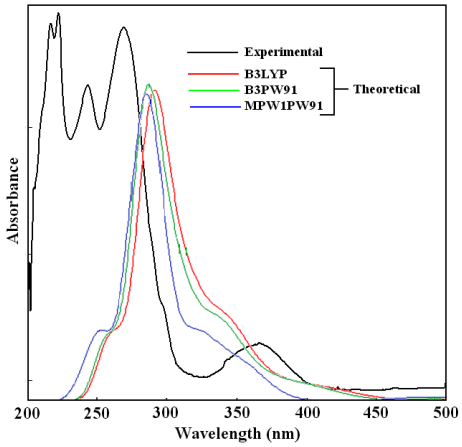

Fig. 30S. Experimental (black line) and theoretical (red, green and blue line, using B3LYP, B3PW91, MPW1PW91 functionals, respectively) electronic spectra of complex **1**.

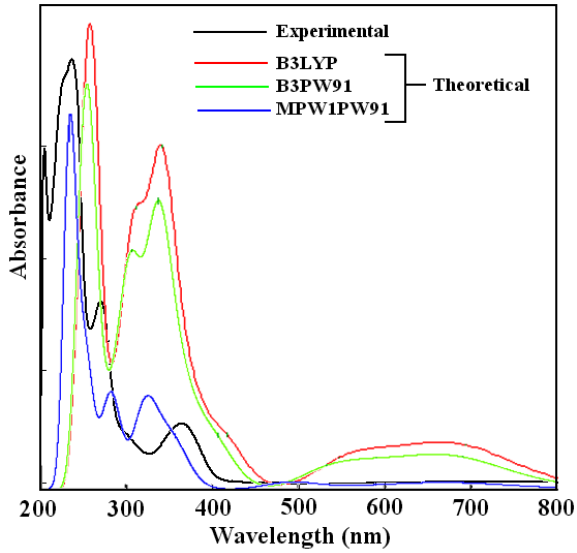

Fig. 31S. Experimental (black line) and theoretical (red, green and blue line, using B3LYP, B3PW91, MPW1PW91 functionals, respectively) electronic spectra of complex **2**.

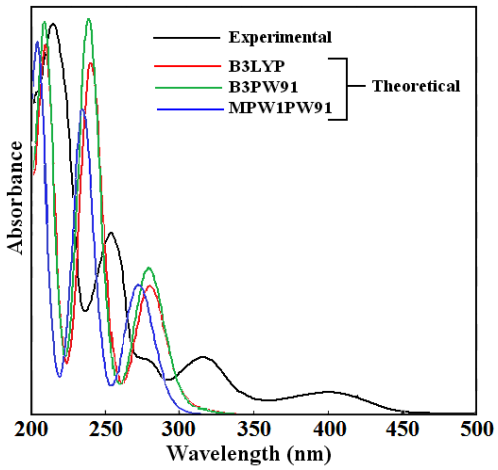

Fig. 32S. Experimental (black line) and theoretical (red, green and blue line, using B3LYP, B3PW91, MPW1PW91 functionals, respectively) electronic spectra of HL.

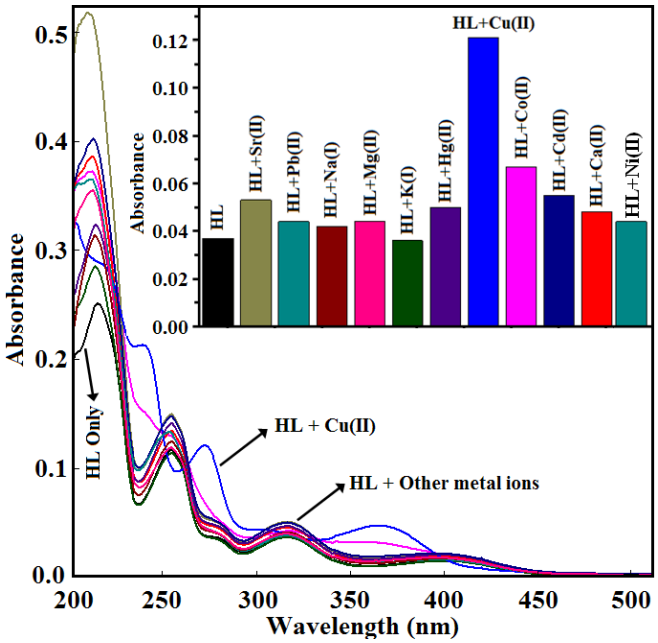

Fig.33S. UV-Vis spectra of 3 ml 0.98µM methanolic solution of HL upon addition of 150 µl 25.66 µM methanolic solution of various metal ions keeping the anion fixed (nitrate in the present case) [inset bar diagram represent the absorbance at 272 nm].

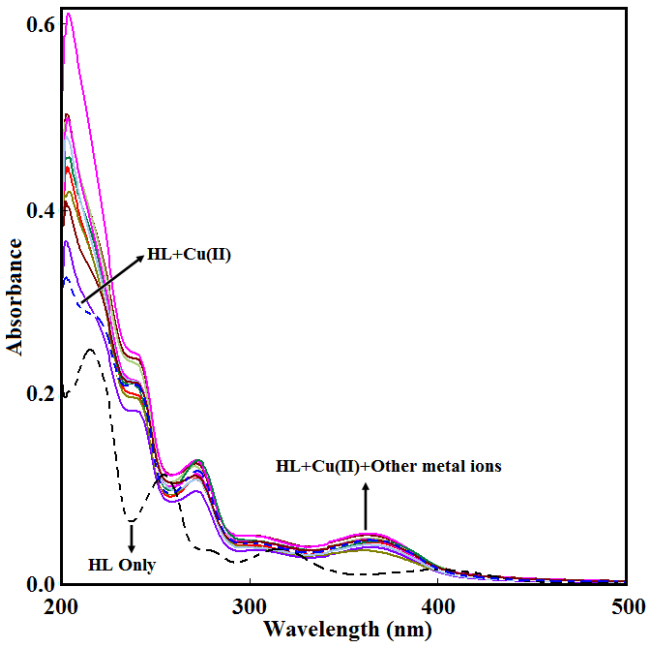

Fig.34S. UV-Vis spectra of adduct containing 3 ml 0.98µM methanolic solution of HL and 150 µl 25.66 µM methanolic solution of Cu(II) ion upon addition of 150 µl 25.66 µM methanolic solution of different metal ions keeping the anionic unit fixed (nitrate in the present case).

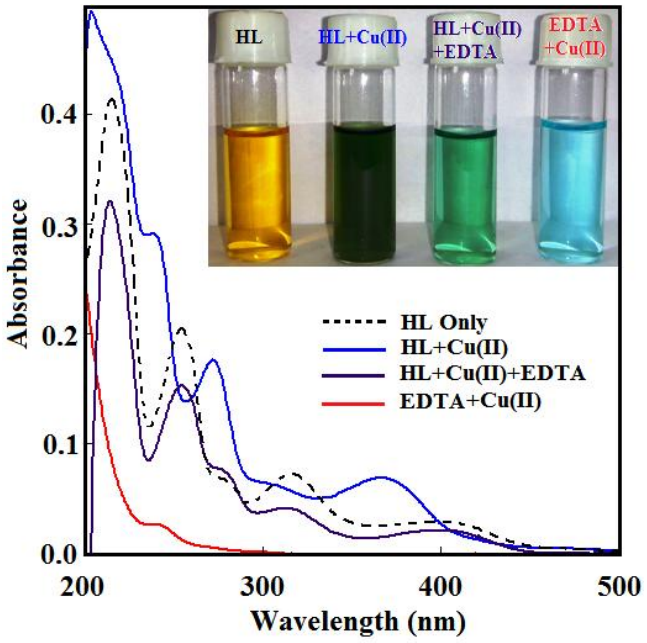

Fig. 35S. UV-vis absorption spectra of HL with $Cu(NO_3)_2 \cdot 3H_2O$. In presence and absence of EDTA.

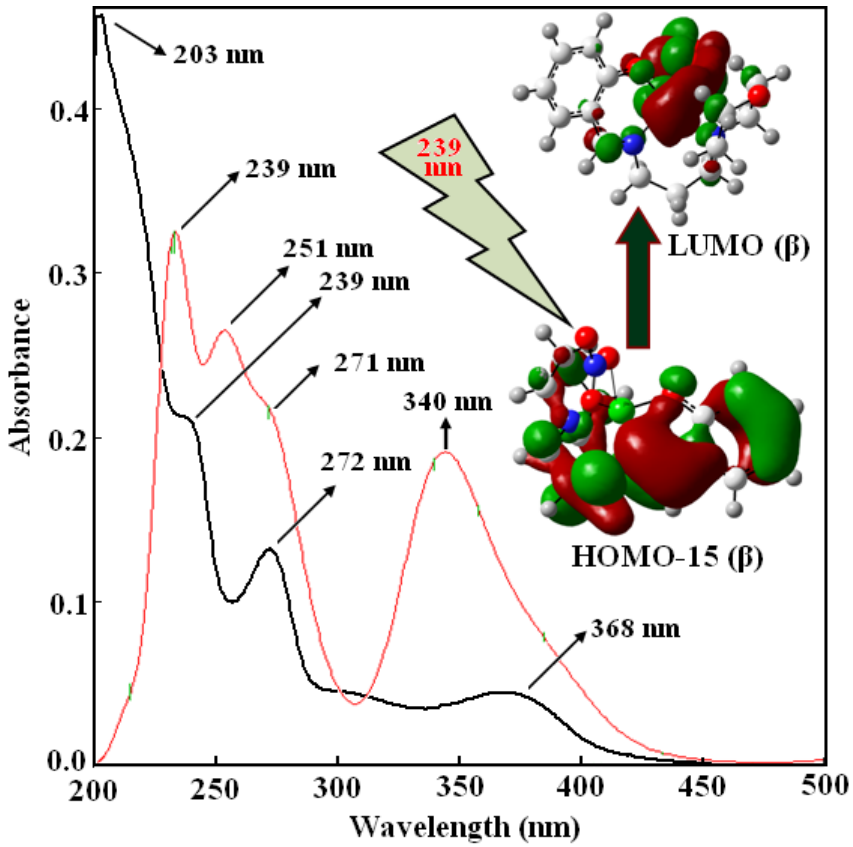

Fig.36S. Theoretical and experimental absorbance spectra of model compound.

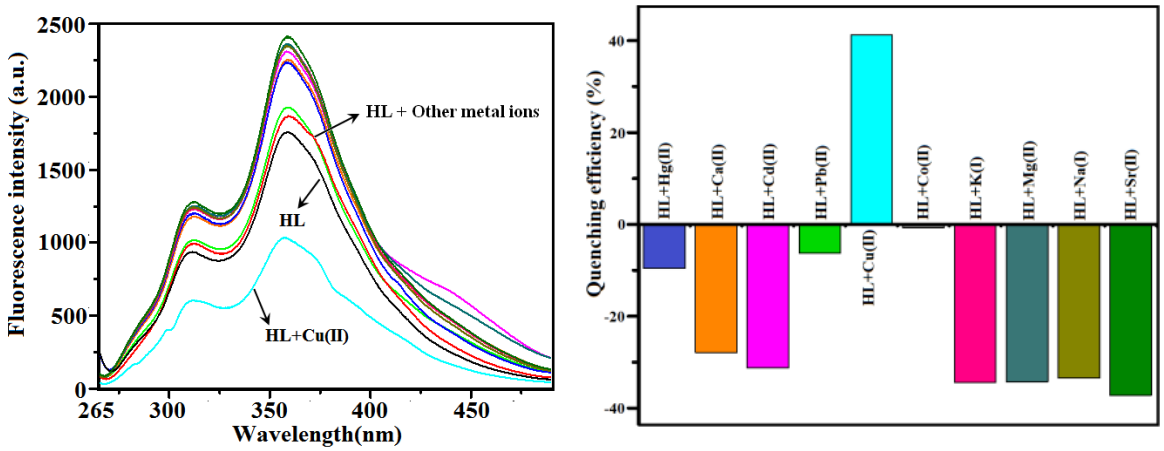

Fig.37S. Left fluorescence behavior of 3 ml 0.1 mM methanolic solution of HL upon addition of 50 µl 0.025(M) methanolic solution of various metal ions keeping the anion fixed (nitrate in the present case), right bar diagram represent the quenching efficiency of various metal ions (negative value indicate enhancement efficiency).

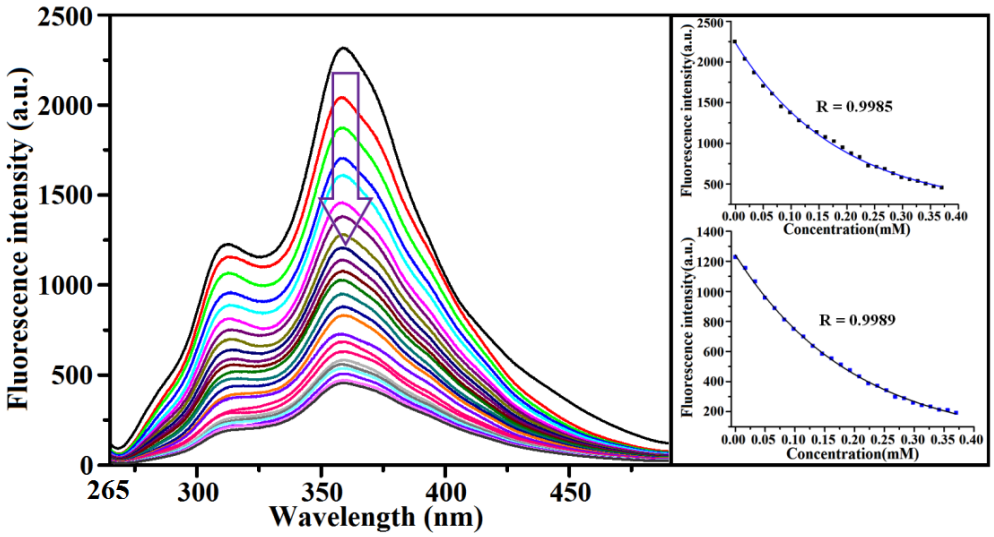

Fig.38S. Fluorescence of 3 ml 0.1 mM methanolic solution of HL upon gradual addition of 10 µl 5 mM methanolic solution of Cu(II) ion keeping the anion fixed (nitrate in the present case) [Inset (a) represent decrease of fluorescence intensity upon gradual addition of Cu(II) at 359nm whereas (b) represent that at 313 nm].

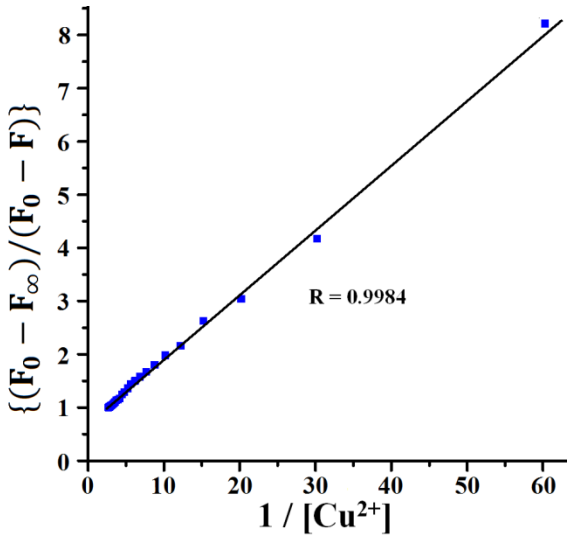

Fig.39S. Benesi-Hildebrand plot with respect to the emission band at 359 nm.

MOs	B3LYP	B3PW91	MPW1PW91
HOMO	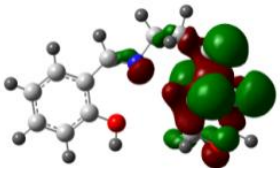 E = -5.79 eV Composition: Morpholine 96%,Imine 3%,Aromatic 1%,Hydroxyl 0%	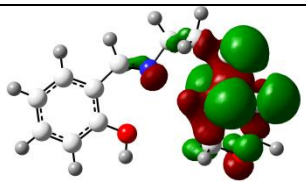 E = -5.87 eV Composition: Morpholine 97%,Imine 2%, Aromatic 1%,Hydroxyl 0%	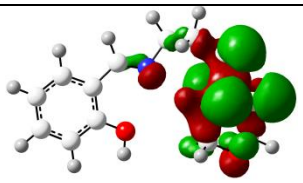 E = -6.12 eV Composition: Morpholine 96%,Imine 2%, Aromatic 1%,Hydroxyl 1%
LUMO	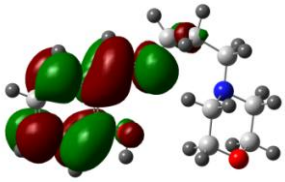 E = -1.13 eV Composition: Morpholine 3%,Imine 39%,Aromatic 57%,Hydroxyl 1%	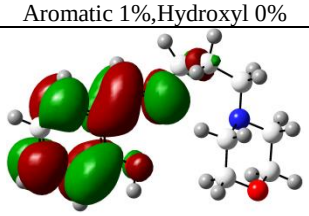 E = -1.23 eV Composition: Morpholine 3%,Imine 39%,Aromatic 57%,Hydroxyl 2%	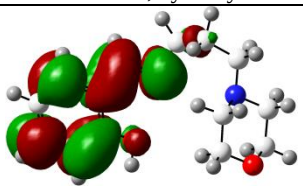 E = -1.02 eV Composition: Morpholine 3%, Imine 38%,Aromatic 57%,Hydroxyl 2%

Fig.40S. Surface plot of frontier orbitals along with their energies and compositions of **HL** using B3LYP, B3PW91 and MPW1PW91 functionals.

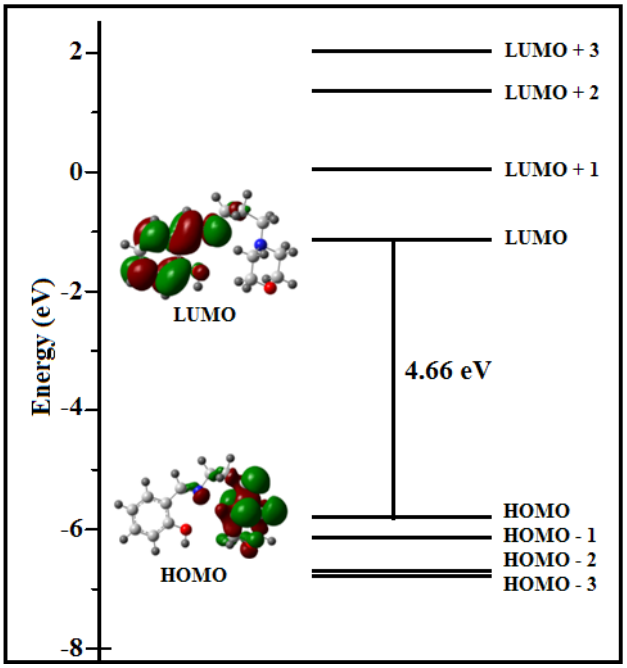

Fig.41S. Calculated molecular orbital energy level diagram of **HL** [B3LYPfunctional; basis set 6-31G(d-p), using conductor-like polarizable continuum model (CPCM) in methanol].

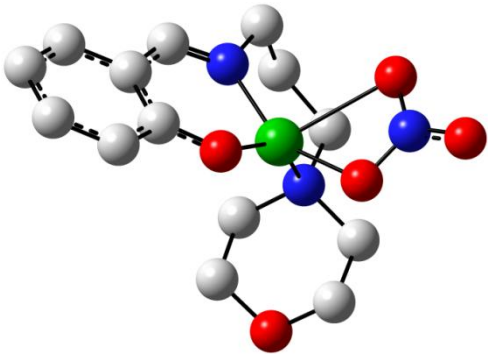

Fig.42S. Optimized structure of model compound

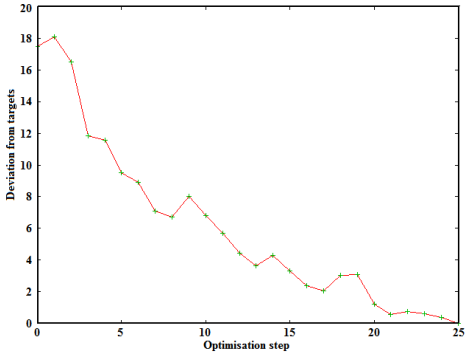

Fig.43S. Deviation from target vs. optimization step of **1 [**using conductor-like polarizable continuum model (CPCM) in methanol; basis set, LanL2DZ].

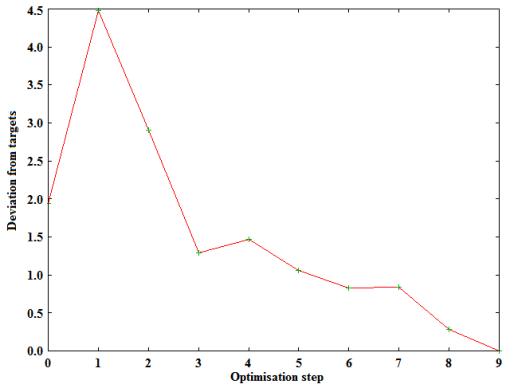

Fig.44S. Deviation from target vs. optimization step of **2 [**using conductor-like polarizable continuum model (CPCM) in methanol; basis set, LanL2DZ].

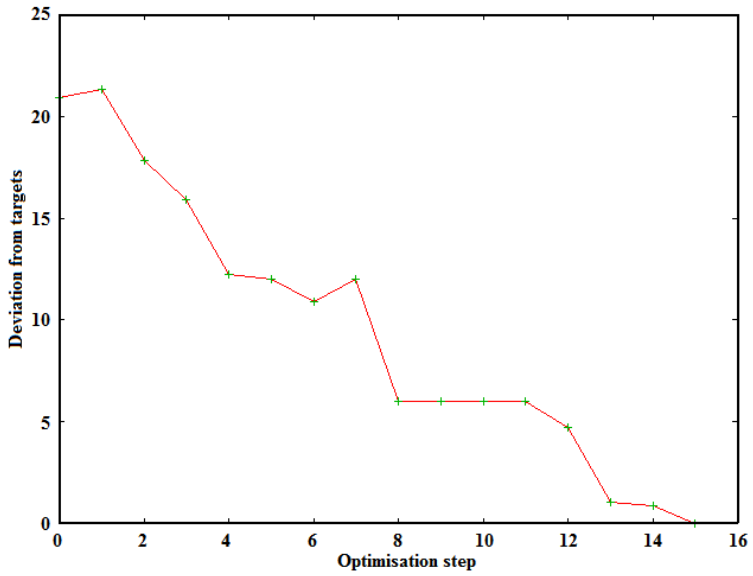

Fig.45S. Deviation from target vs. optimization step of HL [using conductor-like polarizable continuum model (CPCM) in methanol; basis set, 6-31G(d-p)].